I&EC research
Industrial & Engineering Chemistry Research

ARTICLE

pubs.acs.org/IECR

A Mechanism for the Occurrence of Ions in Distilled Water

Ramesh Balakrishnan,† Ravi Sankannavar, and K. Kesava Rao*

Department of Chemical Engineering, Indian Institute of Science, Bangalore -560012, India

ABSTRACT: Solar distillation can be used to produce potable water from contaminated water. However, studies show that ions such as F^- and NO_3^- occur in distillates from solar stills. In order to understand the reasons for this behavior, imaging and distillation experiments were conducted. White dots were seen in the vapor space above the interface of hot water poured into containers. The concentrations of various ions such as F^- and SO_4^{2-} in the distillates from thermal and solar distillation experiments were roughly comparable when the feed consisted of deionized water and also solutions having fluoride concentrations of 100 and 10 000 mg/L. These observations suggest that aerosols enter the distillation setup through leaks and provide nuclei for the condensation of water vapor. The water-soluble component of aerosols dissolves in the drops formed, and some of the drops are transferred to the distillate by buoyancy-driven convection.

INTRODUCTION

About one billion people lack access to clean water,[1] as the water has chemical or microbial contaminants. One of the methods that has been used to produce potable water from contaminated water is solar distillation (see, for example, the work of Gomkale,[2] El-Nashar,[3] and Tiwari et al.[4]). Studies on defluoridation or removal of excess fluoride show that distillates from solar stills contain ions.[5−7] It is surprising that the distillate contained ions such as F^- and Na^+, even though the temperature of the feedwater was well below its boiling point.

The present work aims to examine the mechanisms by which ions are transferred from the feed to the distillate. In the context of thermal distillation, the following mechanisms have been suggested. (i) Some of the feed may be transferred to the distillate in the form of a film of water.[8] The film may flow toward the condenser because of capillarity and the flow of vapor. (ii) Material may be transferred from the surfaces of the distillation apparatus that are in contact with the distillate and from the bottles used for sample storage.[9,10] (iii) The feed may be entrained by the bursting of vapor bubbles at the gas−liquid interface.[8,11]

Experiments designed to test mechanisms i and ii are described below. The other mechanism is eliminated by ensuring that the temperature of the feed is much lower than the boiling point of water.

MATERIALS AND METHODS

Imaging. A 200 mL portion of water was heated to 70 °C and poured into a plastic container of size 6 cm × 7.5 cm × 13.3 cm (Figure 1). The container was then covered with a lid. A window of size 1.2 cm × 1.2 cm was cut in one of the walls for imaging, using the setup shown in Figure 2. When the camera is operated at a high aperture, the high exposure of its charge coupled device to light of high intensity may reduce its performance. Therefore, black paper was used to cover the regions of the wall facing the camera. To examine the effect of the material of the container, and hence test mechanism ii (described above), experiments were also conducted using a container having four aluminum faces and two glass faces. The dimensions of the container and the hole were comparable to those of the plastic container. The inner surfaces of the aluminum faces and also the outer surface of the aluminum plate facing the camera were painted black to reduce the reflection of light.

A laser beam from the source was collimated using a cylindrical lens to form a thin sheet of light that passed through the side walls for illumination. A camera was positioned orthogonal to the sheet to capture the light scattered by the particles or droplets in the illuminated region. A timing interface unit was used to synchronize the generation of the laser pulse with the frame capture by the camera. Image acquisition, storage, and processing were done using proVision software. The specifications of the imaging setup are given in Table 1.

The container was 17 and 30.5 cm away from the laser source and the camera, respectively. In the absence of a window, the vapor space could not be clearly seen through the transparent wall as the drops formed on the wall by condensation scattered the incident light. Closed systems were imaged by covering the window with a glass plate of thickness 1 mm. The plate was heated using a lighted matchstick during imaging to avoid the condensation of vapor on its surface.

Thermal Distillation. A 50 mL portion of the feed was taken in a 100 mL glass beaker kept in a Peltier heater (model MCS 100, Spectralab; Figure 3). The wall of the heating cavity in the heater was maintained at 75 °C. Using a thermometer, the temperature of the water in the beaker was found to be 65 °C. Distillation was carried out at a sub-boiling temperature to avoid entrainment of drops formed by the bursting of vapor bubbles at the air−water interface. A plastic funnel was kept over the beaker to provide a surface for the vapor to condense, and the neck of the funnel was plugged using aluminum foil to prevent the escape of vapor. The

Special Issue: Ananth Issue

Received: January 28, 2011
Accepted: June 1, 2011
Revised: May 23, 2011
Published: June 01, 2011

dx.doi.org/10.1021/ie2002022 | *Ind. Eng. Chem. Res.* 2011, 50, 13202–13209

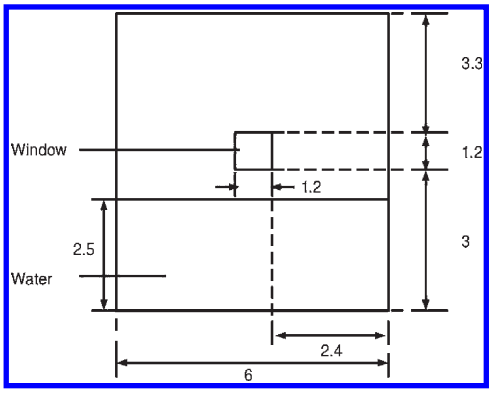

Figure 1. Dimensions of the container used for imaging. All dimensions are in centimeters.

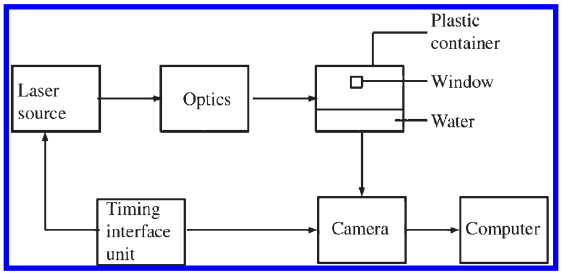

Figure 2. Schematic of the imaging setup.

Table 1. Specifications of the Components of the Imaging Setup

light source:
Nd-YAG laser, dual head pulsed solo-III model, New-Wave Research
operating wavelength: 532 nm, power output: 50 mJ/pulse
camera:
IDT sharp vision model 1400-DE camera with a lens of focal length 60 mm
framing rate: 12 frames/s, resolution: 1360 pixels × 1030 pixels

distillate was collected in a plastic tray made from a sheet used for overhead transparencies (probably a polyester) for a period of 2 h. Using a micropipet, it was then transferred to a polyethylene bottle for storage. To estimate the contribution of ions transferred to the distillate from the surfaces of the funnel, tray, and micropipet, 50 mL of deionized water was heated to 75 °C and 10 mL was used to wash all the parts of the setup that were in contact with the distillate. The washings were collected and analyzed to quantify the background noise in the measurement of the ionic concentrations of samples. The amount of deionized water used for washing was approximately equal to the volume of distillate collected at the end of the batch distillation experiment (10−12 mL).

The experiment described above was repeated using a glass funnel and a stainless steel tray, instead of the plastic funnel and the plastic tray. This modification permits us to examine whether the material of construction of the setup affects the concentration of ions in the distillate.

To study the effect of the concentration of feed, solutions having different concentrations of F^- were prepared by dissolving NaF (minimum assay 97 wt %) in deionized water and were distilled. To study the effect of the quality of ambient air, experiments were

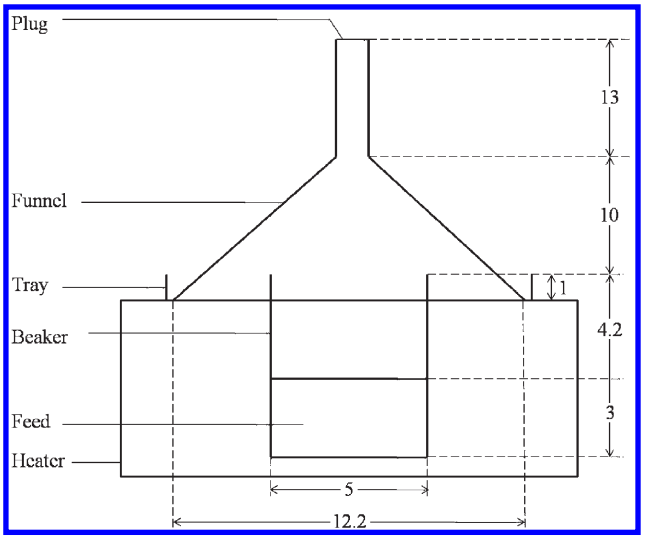

Figure 3. Schematic of a batch distillation setup. All dimensions are in centimeters.

also conducted in a clean room (class 10,000, Four-c-tron) maintained at 21 °C and a relative humidity of 60%. The class of a clean room is the number of particles of size >0.3 μm in volume of 1 m^3.

As the composition of the plastic funnel used in the setup above was not known, a setup made of plexiglas, i.e., poly(methyl methacrylate) was used (Figure 4). A hole of cross sectional area ≈5 cm^2 was cut in one of the walls. To check the effect of the leak area available for the ambient air to enter the vapor space, 100 mL of tap water were distilled when the hole was open and also when it was sealed using parafilm. Tap water was used as feed in place of deionized water as it contains a lower amount of volatile contaminants.[11] In this setup, when the hole was sealed, the distillate was not exposed to the ambient air during the duration of the experiment. Further, the contamination of the distillate due to its contact with the walls is likely to be less than in the earlier setup (Figure 3).

Concentrations of F^-, Cl^-, NO_3^-, and SO_4^{2-} ions in the samples were measured using ion chromatography (Dionex DX 600). Concentrations of Na, K, Ca, and Si were measured using an ICP (inductively coupled plasma) emission spectrometer (iCAP 6000 Series, Thermo Scientific). It is assumed that the concentrations of the first three elements represent the concentrations of the cations Na^+, K^+, and Ca^{2+}, respectively, in the samples.

Solar Distillation. Batch distillation was also done in a solar still (Figure 5 and Table 2). The still consisted of an inclined basin covered by a glass plate. The still was kept in an inclined position to allow the distillate to flow and fall into the collecting duct and to increase the incident flux of solar radiation. Feed solutions having various concentrations of F^- were prepared using deionized water and 300 mL portions were distilled.

RESULTS AND DISCUSSION

Imaging. A 100 mL glass beaker was completely filled with water whose initial temperature was 70 °C. The beaker was left open to the atmosphere. Images of the region above the air−water interface show white dots (Figure 6). Perhaps these dots are drops formed by the heterogeneous nucleation of water vapor

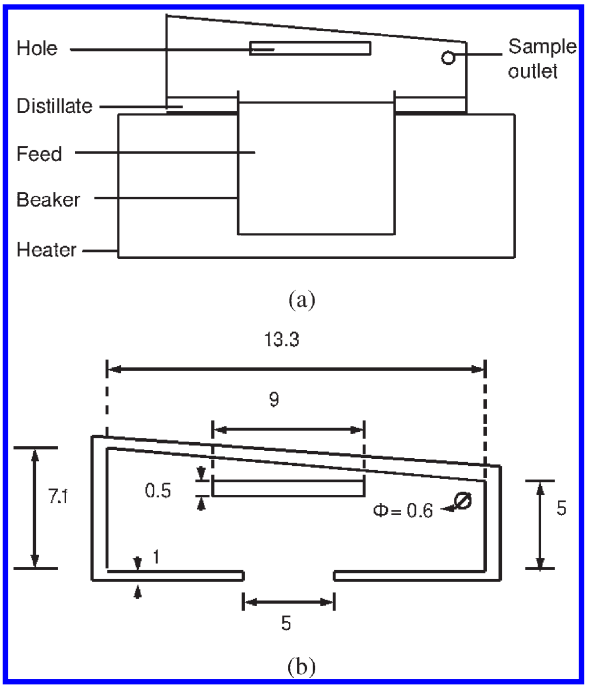

Figure 4. (a) Schematic and (b) dimensions of an alternative batch distillation setup. All dimensions are in centimeters.

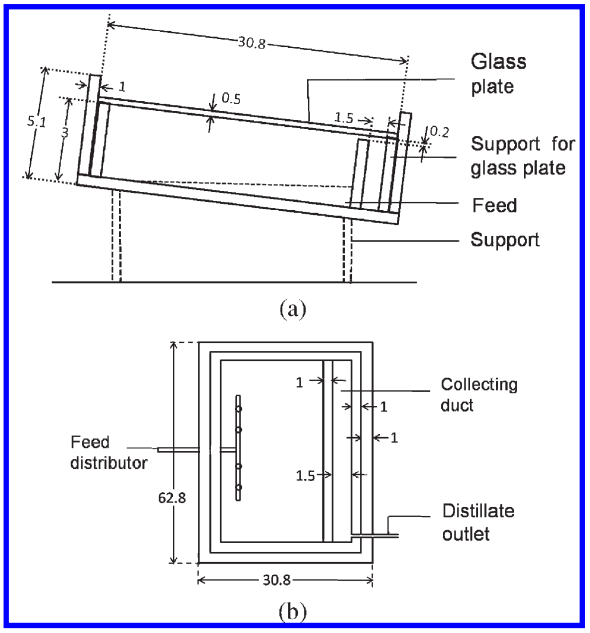

Figure 5. (a) Elevation and (b) plan view of the solar still. All dimensions are in centimeters.

on the surfaces of aerosols. Homogeneous nucleation is not expected to occur as it requires a high degree of supersaturation.

Before proceeding further, a brief introduction to atmospheric aerosols and their ionic content may be helpful. Aerosols are fine solid particles dispersed in the ambient air.[12] They are formed by processes such as evaporation of entrained droplets, gas to particle conversion by reaction or sublimation, incomplete combustion of fuels, and mechanical disintegration of solids by operations such as crushing and grinding. Table 3 shows the ionic

Table 2. Specifications of the Still

surface area	0.19 m^2
maximum feed capacity	1.75 L
inclination	≈7° from horizontal
location	placed on the terrace of our department, facing south

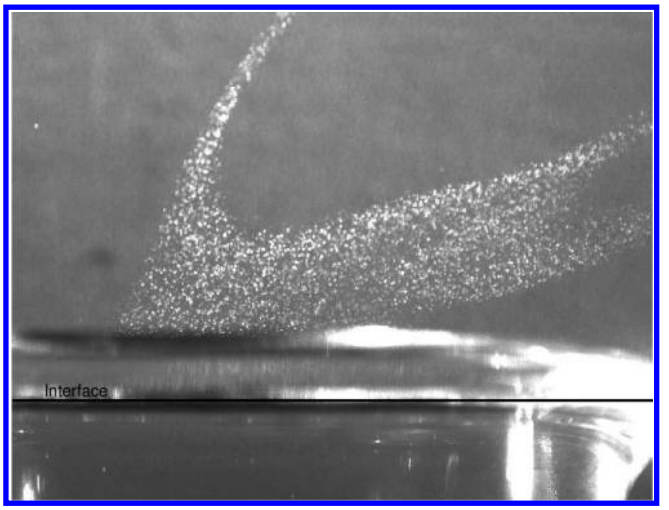

Figure 6. Image of the region above the air−water interface in a beaker filled with water: (parameter values) initial temperature of the water = 70 °C, aperture of the camera = $f/16$, where f = 60 mm is the focal length, field of the image frame ≈50 mm × 30 mm.

composition of particles of size less than 2.5 μm, determined by sampling the air in Mumbai, India. It is likely that the water-soluble component of aerosols is one of the sources of ions in the distillate.

Plumes rising from hot coffee and trails of a jet plane in a clear sky are common examples of the condensation of vapor on aerosols. Wet scrubbers used to remove aerosols and laser counters used to estimate the number of cloud condensation nuclei are based on this principle. Schaber[13] studied the effect of aerosols on the performance of a gas−liquid contact scrubber. Under identical operating conditions, the removal of HCl from a feed containing aerosols was less than that from the feed that did not have aerosols. Some of the drops formed by heterogeneous nucleation on the aerosols were entrained by the exhaust gas, leading to a lower removal of HCl.

The large number of dots observed (Figure 6) may correspond to the high number density of aerosols in urban air (≈10^5−4 × 10^6 cm^{-3}).[12] Dots were observed even when the initial temperature of water was 55 °C, but the frequency of their appearance in the sequence of images decreased with the temperature.

A 200 mL portion of water was heated to 70 °C and poured into a plastic container. White dots were observed in the vapor space between the surface of the water and the lid of the container (Figure 7a), analogous to the dots observed above the beaker (Figure 6). When water at room temperature was poured into the container, the dots were absent (Figure 7b). As the humidity of the vapor space above the water surface was not high enough to cause heterogeneous nucleation on aerosols, no drops were formed.

White dots were observed in all the 200 images captured through the open window at a rate of 12 frames per second. This

Table 3. Ionic Concentration of the Ambient Air in Mumbai, Measured during 2003−2004[a]

ionic concentration of air ($\mu g/m^3$)	F^-	Cl^-	NO_3^-	SO_4^{2-}	Na^+	K^+	Ca^{2+}	Mg^{2+}
mean	0.3	4.62	0.97	11.44	3.15	2.85	2.73	0.97
standard deviation	0.18	2.24	0.84	8.56	1.53	1.45	1.07	0.52

[a] Data of Kumar et al.[17]

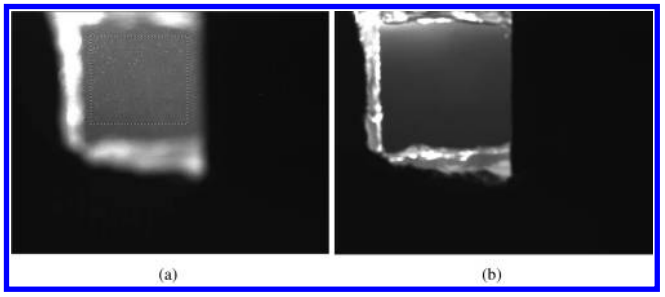

Figure 7. Images of the region between the surface of the water and the lid of the plastic container, taken through the open window. The initial temperature of the water was 70 °C (a) and room temperature (≈27 °C) (b). The rectangle marked by broken lines in a contains 158 422 pixels and represents the region used for calculating average grayscale intensity I_g. The setup shown in Figure 1 was used: (parameter value) aperture of the camera = $f/4$, where f = 60 mm is the focal length.

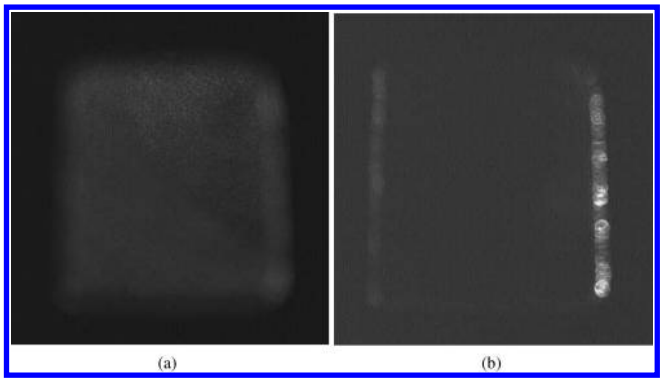

Figure 8. Images of the region between the surface of the water and the lid of the container with aluminum and glass faces, taken through the open window. The initial temperature of the water was 70 °C (a) and room temperature (≈26 °C) (b). The setup shown in Figure 1 was used: (parameter value) aperture of the camera = $f/4$, where f = 60 mm is the focal length.

feature was absent in the images captured through a heated glass window. Here the haziness of the vapor space decreased as the time increased (Figure 9). To quantify the decrease in the haziness, the average grayscale intensity I_g of the marked region (Figure 9) was calculated using the Adobe Photoshop software. The number of pixels in the marked region for the open and closed windows were 158 422 and 88 312, respectively. When the window was closed, I_g decreased with the image number of the sequence n, or equivalently, the time (Figure 10). In contrast, I_g remained approximately constant when the window was open.

For the closed window, scavenging of the aerosols that were initially present in the vapor space may cause I_g to decrease with time. This process involves the formation of drops by heterogeneous nucleation of water vapor on the aerosols, and their removal from the vapor space by deposition on the walls of the

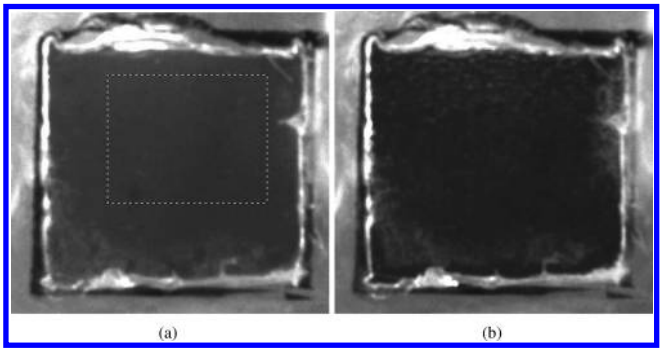

Figure 9. Images of the region between the water surface and the lid of the container, taken through the closed window. The image number was 1 (a) and 200 (b). The rectangle marked by broken lines in (a) contains 88 312 pixels and represents the region used for calculating average grayscale intensity I_g. The setup shown in Figure 1 was used: (parameter values) initial temperature of the water = 70 °C, aperture of the camera = $f/4$, where f = 60 mm is the focal length, frame rate = 12 frames/s.

container or on the surface of the pool of water. For the open window, the removal of aerosols was compensated by the entry of fresh aerosols through the window. Hence I_g remained approximately constant.

The experiments described above were repeated using the container with aluminum and glass faces instead of the plastic container. The results obtained with both the containers were qualitatively similar. White dots were visible in the images taken through the open window (Figure 8a) when the initial temperature of the water was 70 °C, as in the corresponding images for the plastic container (Figure 7a). With water at room temperature, no dots were observed (Figure 8b), as in the earlier case (Figure 7b).

Thermal Distillation. *Effect of the Feed Concentration.* Let c_a denote the concentrations of anions such as F^- and SO_4^{2-}, and c_c the concentration of cations such as Na^+ and Ca^{2+}. The subscripts "d" and "f" will be used to refer to the concentrations in the distillate and feed, respectively. Thus, c_{ad} denotes the concentration of anions in the distillate.

Using the batch distillation setup shown in Figure 3, deionized water and water containing fluoride were distilled. The background noise (Table 4) is a measure of the contamination of samples due to handling and the experimental setup; data for this case were generated by analyzing the samples obtained by washing the setup with 12 mL of deionized water. The concentrations of F^- and SO_4^{2-} in the distillate differed from the background noise, whereas that of Cl^- was comparable to it (Table 4). It is difficult to quantify the differences or similarities between the distillate and the background noise more precisely, as the measured concentrations varied widely. For example, consider the concentration of Cl^- in the distillate, when deionized water was used as the feed. If 95% confidence limits are calculated using the data shown in Table 4, the lower confidence limit turns out to be negative. The problem can be addressed by analyzing a larger number of

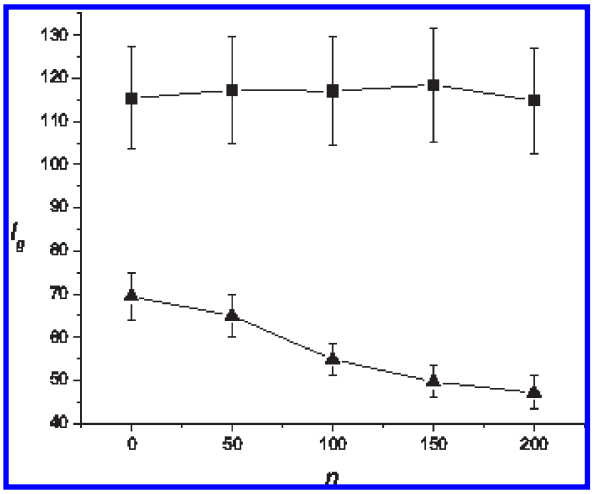

Figure 10. Variation of the grayscale intensity I_g with the image number of the sequence n for the open window (■) and the closed window (▲). The values $I_g = 0$ and $I_g = 255$ denote black and white, respectively. The error bars represent the standard deviation of the grayscale intensities of the pixels in the marked regions in Figures 7a and 9a.

samples; however, as the ion chromatograph was not located in our department, there were constraints on the number of samples that could be analyzed.

Considering F^-, the values of c_{ad} were comparable when the feed consisted of (i) deionized water whose fluoride concentration $c_{F,f}$ was below the limit of quantitation (0.02 mg/L) and (ii) a solution with $c_{F,f} = 100$ mg/L (Table 4). For $c_{F,f} = 10\,000$ mg/L, the values of c_{ad} were higher, but the scatter was larger compared to $c_{F,f} = 100$ mg/L.

The distillate contained not only the ions present in the feed, but also other species such as Cl^-, SO_4^{2-}, and NO_3^-. Further, in the chromatogram corresponding to the distillate, there was no peak corresponding to Br^-, an anion that is usually absent in ambient air.[12]

Overall, these results suggest that there is a distinct source of contamination of the distillate, over and above any transfer of ions from the feed to the distillate. As mentioned earlier, the water-soluble component of aerosols could be the source of the contaminants.

Effect of the Quality of the Air. To study the effect of the quality of the ambient air on the concentration of ions in the distillate, deionized water was distilled inside a clean room. The concentrations of cations in the distillate c_{cd} were roughly comparable for samples distilled inside and outside the clean room (Table 5). The air enters the clean room through a high efficiency particulate air (HEPA) filter that removes most of the particles larger than 0.3 μm. Hence, it appears that aerosols smaller than 0.3 μm contribute to the contamination of the distillate.

For Na^+ and K^+, the values of c_{cd} show a larger scatter for samples distilled outside the clean room than for those distilled inside the room (Table 5). This result is consistent with the high temporal variation observed for the concentration of atmospheric aerosols. For example, the aerosol mass per unit volume of air, measured at Bangalore[14] from September 2005 to February 2006, varied from 10 to 160 $\mu g/m^3$, with a mean value of 70 $\mu g/m^3$.

Effect of the Material of the Funnel and the Tray. Table 6 shows the results obtained when deionized water was distilled

Table 4. Variation of the Concentration of Anions in the Distillate c_{ad} with the Concentration of F^- in Feed $c_{F,f}$[a]

	c_{ad} (mg/L)			
$c_{F,f}$ (mg/L)	F^-	Cl^-	SO_4^{2-}	NO_3^-
background	< c_D	0.25	< c_D	< c_D
noise	< c_D	0.16	< c_D	< c_D
	< c_D	0.29	< c_D	< c_D
deionized	0.06	0.22	0.13	< c_Q
water	0.05	1.09	0.35	0.05
	0.05	0.55	0.48	0.08
100	0.04	0.29	0.24	0.04
	0.05	0.26	0.23	0.06
	0.04	0.24	0.18	0.02
10,000	0.09	0.47	0.43	0.09
	0.11	0.9	0.75	0.23
	0.37	0.37	0.18	0.06
c_D (mg/L)	0.006	0.01	0.03	0.02
c_Q (mg/L)	0.02	0.04	0.1	0.06

[a] Each row represents the results of an independent experiment performed using the setup shown in Figure 3. Here c_D and c_Q denote the limits of detection and quantitation, respectively, estimated as described in the Appendix. The measurements were done using ion chromatography.

using (i) a plastic funnel and a plastic tray and (ii) a glass funnel and a stainless steel tray. For the background noise, the concentrations of the cations were roughly comparable, but the values were slightly larger for Na^+ and K^+ for some of the trials with the setup i. The experiments conducted outside the clean room show similar trends. Experiments could not be conducted inside the clean room, as the compressor that supplied air to it broke down. It appears that material of construction of the setup does not significantly affect the concentrations of the ions in the distillate, at least for the two setups used.

Effect of the Leak Area. Using the setup shown in Figure 4, tap water was distilled when the hole was open and also when it was closed. As in the other experiments, deionized water was used to wash the setup for the measurement of the background noise. The concentrations of cations in the distillate c_{cd} were roughly comparable in both cases (Table 7). However, the scatter in the data was less in the latter case, probably because aerosols could not enter the system when the hole was closed.

Weber et al.[15] estimated the chemical composition of the water-soluble component of aerosols using an instrument called the particle-into-liquid sampler (PILS). Ambient air passing through a filter of pore size 2.5 μm was mixed with steam to promote the condensation of vapor on the aerosols. The drops formed were collected using an impactor plate. Ultrapure water was used to wash the plate, and the washings were analyzed for ions. The flow rates of the ambient air $\dot{Q}_A$ and the wash liquid $\dot{Q}_L$ were 5000 and 0.1 mL/min, respectively. The concentrations c_A of NO_3^- and SO_4^{2-} in the ambient air were 3 and 20 $\mu g/m^3$, respectively. The concentration of ions in the wash liquid c_L is given by

$$c_L = \frac{c_A \dot{Q}_A}{\dot{Q}_L} \quad (1)$$

Using eq 1, the values of c_{L,NO_3^-} and $c_{L,SO_4^{2-}}$ were found to be 0.15 and 1 mg/L, respectively. These values are comparable to

Table 5. Variation of the Concentration of Cations in the Distillate c_{cd} with the Quality of the Ambient Air[a]

	c_{cd} (mg/L)		
sample	Na	K	Si
background	0.070	0.032	0.004
noise	0.038	0.030	0.014
	0.052	0.023	0.004
inside	0.113	0.070	0.030
clean room	0.104	0.040	0.014
	0.086	0.035	0.018
outside	0.044	0.053	0.045
clean room	0.124	0.059	0.030
	0.284	0.207	0.028
c_D (mg/L)	0.004	0.007	0.004
c_Q (mg/L)	0.009	0.01	0.007

[a] Each row represents the results of an independent experiment performed using the setup shown in Figure 3. Here c_D and c_Q denote the limits of detection and quantitation, respectively, estimated as described in the Appendix. The column labelled Si probably represents neutral species. The measurements were done using atomic emission spectrometry. The wavelengths (in nanometers) of the lines used were Na (589.592), K (766.490), and Si (212.412). The experiments were conducted during the period January 7−10, 2010.

Table 6. Effect of the Material of the Funnel and the Tray on the Concentration of Cations in the Distillate c_{cd}: gs, glass funnel and stainless steel tray; p, plastic funnel and plastic tray[a]

	c_{cd} (mg/L)					
sample	Na		K		Si	
	gs	p	gs	p	gs	p
background	0.10	0.17	< c_D	< c_D	0.03	0.03
noise	0.05	0.06	0.07	< c_D	0.02	0.02
	0.01	0.14	< c_D	0.18	<0.01	0.02
outside	0.11	0.08	0.17	< c_D	0.09	0.11
clean room	0.09	0.08	0.07	< c_D	0.06	0.09
	0.06	0.32	0.07	0.46	0.05	0.08
c_D (mg/L)	0.01	0.01	0.06	0.06	0.01	0.01
c_Q (mg/L)	0.03	0.03	0.1	0.1	0.02	0.02

[a] Each row represents the results of an independent experiment performed using the setup shown in Figure 3. Here c_D and c_Q denote the limits of detection and quantitation, respectively, estimated as described in the Appendix. The column labelled Si probably represents neutral species. The measurements were done using atomic emission spectrometry. The wavelengths of the lines used were as in Table 5. The experiments were conducted during the period May 14−16, 2011.

the concentrations of NO_3^- and SO_4^{2-} in the distillate obtained in our experiments (Table 4) (0.02−0.08 and 0.13−0.48 mg/L, respectively). This result supports the conjecture that the water-soluble component of atmospheric aerosols may be transferred to the distillate.

Let $c_{Na,a}$ and $c_{Na,d}$ denote the concentrations of Na^+ ions in the ambient air and in the distillate, respectively. Assuming that the ambient air is the only source of contaminants in the distillate, the velocity v_a of the ambient air that should have entered the

Table 7. Variation of the Concentration of Cations in the Distillate c_{cd} with the Leak Area[a]

	c_{cd} (mg/L)		
sample	Na	K	Ca
background	< c_D	< c_D	0.05
noise	0.05	0.08	0.06
	0.07	0.07	0.09
	< c_D	< c_D	0.04
hole	< c_D	< c_D	0.13
open	< c_D	< c_D	0.06
	0.25	0.17	0.18
	0.12	0.08	0.35
hole	< c_D	< c_D	0.09
closed	0.06	0.05	0.10
	< c_D	< c_D	0.10
	< c_D	< c_D	0.09
c_D (mg/L)	0.04	0.04	0.04
c_Q (mg/L)	0.08	0.08	0.07

[a] Each row represents the results of an independent experiment performed using the setup shown in Figure 4. Here c_D and c_Q denote the limits of detection and quantitation, respectively, estimated as described in the Appendix. The measurements were done using atomic emission spectrometry. The wavelengths (in nanometers) of the lines used were Na (589.592), K (769.896), and Ca (317.933). The experiments were conducted during the period May 3−5, 2010.

vapor space through the hole (Figure 4) is given by

$$v_a = \frac{c_{Na,d} V_d}{c_{Na,a} A_h t_d} \quad (2)$$

where V_d is the volume of the distillate collected in a time t_d, and A_h is the area of the hole. As data on the ionic composition of air at Bangalore were not available, the mean value of $c_{Na,a}$ measured at Mumbai (Table 3) (= 3.15 $\mu g/m^3$) was used. For the parameter values corresponding to the present experiments (area of the hole = 4.5 cm^2, experimental duration = 2 h, V_d = 12 mL, and considering $c_{Na,d}$ values in the range 0.04−0.25 mg/L), $v_a \approx$ 5−29 cm/s. If concentrations corresponding to the K^+ ions are used, $v_a \approx$ 5−22 cm/s. The estimated velocities are not unreasonably large and could have occurred in our experiments.

Vatistas et al.[16] had studied the rate of infiltration of ambient air at −1 °C through automatic doors into a room maintained at 18 °C. They measured an infiltration rate of 617 m^3/h through three doors, each of size 1.65 m × 1.91 m, into a room of size 15.2 m × 2.47 m × 2.15 m. At a steady state, the rate at which warm air leaves the room through the upper part of the door is equal to the rate at which cold ambient air enters the room through the lower part. Allotting half the area of the doors for infiltration, the average velocity of the entering air is estimated to be 4 cm/s, which is also in the range of velocities estimated above. In our system, the efflux of warm vapor from the vapor space, if not compensated by evaporation, could lead to a decrease in the pressure, causing the ambient air to flow into the container. The decrease in pressure caused by the condensation of vapor can also aid infiltration.

Solar Distillation. Using the solar still shown in Figure 5, deionized water and water containing sodium fluoride were distilled. The values of the concentrations of the anions c_{ad} for SO_4^{2-} and Cl^- ions were much higher than those for F^- and

Table 8. Variation of the Concentration of Anions in the Distillate c_{ad} with Concentration of F^- in feed, $c_{F,f}$[a]

	c_{ad} (mg/L)			
$c_{F,f}$ (mg/L)	F^-	Cl^-	SO_4^{2-}	NO_3^-
deionized	0.02	1.40	4.10	0.15
water	0.02	0.36	1.30	0.07
	0.04	1.22	1.99	0.32
	0.54	2.75	6.15	1.20
10	0.02	1.41	3.41	0.63
	0.31	1.92	4.74	0.65
c_D (mg/L)	0.006	0.01	0.03	0.02
c_Q (mg/L)	0.02	0.04	0.1	0.06

[a] Each row represents the results of an independent experiment performed using the solar still (Figure 5). Here c_D and c_Q denote the limits of detection and quantitation, respectively, estimated as described in the Appendix. The measurements were done using ion chromatography. The experiments were conducted during the period from October 15, 2009 to January 21, 2010.

NO_3^- (Table 8). The data of Kumar et al.[17] on the ionic concentration of air follows the same trend (Table 3).

It is instructive to compare the results obtained for experiments done using the laboratory setup (Figure 3) and the solar still (Figure 5). Even though much higher feed concentrations were used in the former case (Table 4), the values of c_{ad} were invariably higher in the latter case (Table 8). This trend may be caused by the larger leak area and the longer duration of the experiments (≈6 h) for the solar still. These factors are conducive to the entry of a larger number of aerosols into the system and hence into the distillate, leading to higher values of c_{ad}.

Dry Deposition of Aerosols. A 10 mL portion of deionized water was taken in polyethylene bottles, which were left open to the atmosphere for intervals ranging from 2 to 24 h. The concentrations of anions in these samples were less than the corresponding limits of detection. Hence, dry deposition of aerosols does not appear to be a significant source of contaminants.

Proposed Mechanism of Contamination. Evaporation leads to a high concentration of water vapor in the region between the upper surface of the feed and the condenser surface. The vapor condenses on the aerosols that are transported into the vapor space by the ambient air that enters the system through leaks. The water-soluble component of the aerosols dissolves in the drops formed, which may be convected by buoyancy-driven currents onto the film of distillate formed on the condenser plate.

CONCLUSIONS

Imaging and thermal and solar distillation experiments suggest that drops are formed by the heterogeneous nucleation of vapor on the surfaces of aerosols present in the ambient air. Free convection in the vapor space causes some of the drops to be deposited in the distillate, and the water-soluble component of the aerosols provides one of the sources of ions. The direct transfer of ions from the feed to the distillate seems unlikely, as there was no correlation between the concentrations of F^- in the two phases. Thermal distillation experiments conducted using a (i) plastic funnel and a plastic tray and (ii) glass funnel and a stainless steel tray suggest that the material of construction fo the setup does not significantly affect the concentration of ions in the distillate. This observation is in accord with the hypothesis that aerosols are the sources of ions.

APPENDIX: LIMITS OF DETECTION AND QUANTITATION

The limit of detection c_D is the smallest concentration of the analyte that can be detected with reasonable certainty.[18] The limit of quantitation c_Q is the concentration above which quantitative results can be obtained with a specified degree of confidence.[18] As noted by Mermet,[19] there are no unique estimates of c_D and c_Q.

(i) ICP-Atomic Emission Spectrometry. Here we use estimates based on the prediction bands associated with the linear regression line of the calibration data.[19] Let (X_i, Y_i) denote the concentration and intensity, respectively, corresponding to the ith data point, n the number of data points, $\overline{X} \equiv (\sum_{i=1}^{n} X_i)/n$ and $\overline{Y} \equiv (\sum_{i=1}^{n} Y_i)/n$ the mean values of $\{X_i\}$ and $\{Y_i\}$, respectively, $x_i \equiv X_i - \overline{X}$, and $y_i \equiv Y_i - \overline{Y}$.

The estimates of c_Q and c_D are given by

$$c_Q = \frac{2t_{\alpha,n-2}S}{b_1}\left[\frac{\overline{X}^2}{\sum_{i=1}^{n} x_i^2} + \frac{1}{m} + \frac{1}{n}\right]^{1/2} \quad ; \quad c_D = \frac{c_Q}{2} \qquad (A.1)$$

where $t_{\alpha,n-2}$ is the test static obtained from the Student's t-distribution for a level of significance α and $n-2$ degrees of freedom and S is the standard deviation about the regression line $\hat{Y} = b_0 + b_1 X$, given by

$$S = \sqrt{\frac{\sum_{i=1}^{n}(Y_i - \hat{Y}_i)^2}{n-2}} = \sqrt{\frac{\sum_{i=1}^{n} y_i^2 - b_1^2 \sum_{i=1}^{n} x_i^2}{n-2}} \qquad (A.2)$$

Here

$$b_1 = \frac{\sum_{i=1}^{n} x_i y_i}{\sum_{i=1}^{n} x_i^2} \qquad (A.3)$$

is the slope of the regression line, and m is the number of observations used to estimate the concentration of an unknown sample. In the present work, $\alpha = 0.05$ and $m = 3$. Equation A.1 is a simplified version for a more accurate equation; it can be used when $c_Q \ll \overline{X}$.

Let s denote the standard deviation corresponding to the intensities $\{Y_i\}$ of replicates at a given value of X. Equation A.1 is based on the assumption that s is independent of the intensity, which does not hold in most atomic spectroscopy methods.[19] More accurate estimates of c_D and c_Q can be obtained by weighting,[19] with the weights chosen being proportional to $1/s$, $1/s^2$, $1/Y_*$, or $1/Y_*^2$, where Y_* denotes the average intensity of the replicates.[20] As only three replicates were used for each value of X in the present experiments, the values of s are not very reliable. In some cases, the average intensity Y_* corresponding to the blank was negative, precluding the use of $1/Y_*$ as the weight. Calculations show that the present unweighted estimates of c_D and c_Q, given by eq A.1, are conservative, i.e., they are larger than the weighted estimates. This trend is consistent with the results reported by Mermet.[20]

(ii) Ion Chromatography. The chromatogram is a plot of the electrical conductance G versus the time. For the instrument used in the present work, the amplitude of the signal corresponding to the background noise was ≈0.002 μS. The conductances G_D and G_Q corresponding to the limits of detection and quantitation, respectively, were estimated as[21]

$$G_D = 3 \times 0.002 = 0.006\ \mu S;$$
$$G_Q = 10 \times 0.002 = 0.02\ \mu S$$

The height of the Cl^- peak corresponding to a concentration of 51.8 μmol/L was 1.083 μS. As both the height of the peak and its area varied linearly with the concentration of Cl^- in the range (0−51.8 μmol/L), the values of G_D and G_Q were used to calculate the concentrations corresponding to the limits of detection and quantitation c_D and c_Q, respectively. We obtain c_D = 0.3 μmol/L and c_Q = 1.0 μmol/L. It is assumed that the c_Q and c_D values are applicable to the other anions also.

AUTHOR INFORMATION

Corresponding Author

*E-mail: kesava@chemeng.iisc.ernet.in.

Present Addresses

†Department of Chemical Engineering, University of Houston, Houston, TX 77204-4004, USA.

ACKNOWLEDGMENT

We are grateful to Prof. V. Kumaran for permitting us to use the particle image velocimetry (PIV) setup, Dr. Partha Sarathy Goswami for assistance with the PIV experiments, Dr. Jean Riotte of the Indo-French Water Cell for permitting us to use the ion chromatograph and for the analysis of anions, Mr. Siva Chidambaram and Mr. Saravana for the analysis of cations, Profs. N. V. Joshi and K. S. Gandhi for helpful discussions, and the referees for helpful comments. K.K.R. would like to thank his teacher Prof. M. S. Ananth for being an excellent mentor.

REFERENCES

(1) United Nations Development Programme, *Human Development Report*; Palgrave Macmillan: New York, 2006.

(2) Gomkale, S. D. Operational experience with solar stills in an Indian village and their contribution to the drinking water supply. *Desalination* **1988**, *69*, 177–182.

(3) El-Nashar, A. M. Performance of the solar desalination plant at Abu Dhabi. *Desalination* **1989**, *72*, 405–424.

(4) Tiwari, G. N.; Singh, H. N.; Tripathi, R. Present status of solar distillation. *Solar Energy* **2003**, *75*, 367–373.

(5) Hanson, A.; Zachritz, W.; Stevens, K.; Mimbela, L.; Polka, R.; Cisneros, L. Distillate water quality of a single-basin solar still: laboratory and field studies. *Solar Energy* **2004**, *76*, 635–645.

(6) Anjaneyulu, L. *Defluoridation of Drinking Water and Estimation of Fluoride*. M.E project report, Indian Institute of Science, 2007.

(7) Sahoo, B. B.; Sahoo, N.; Mahanta, P.; Borbora, L.; Kalita, P.; Saha, U. K. Performance assessment of a solar still using blackened surface and thermocol insulation. *Renewable Energy* **2008**, *33*, 1703–1708.

(8) Hughes, R. C.; Murau, P. C.; Gundersen, G. Ultra-pure water. Preparation and quality. *Anal. Chem.* **1971**, *43*, 691–696.

(9) Healy, G. M.; Morgan, J. F.; Parker, R. C. Trace metal content of some natural and synthetic media. *J. Biol. Chem.* **1952**, *198*, 305–312.

(10) Moody, J. R.; Lindstrom, R. M. Selection and cleaning of plastic containers for storage of trace element samples. *Anal. Chem.* **1977**, *49*, 2264–2267.

(11) Petrick, H. J.; Schulze, F. W.; Cammenga, H. K. The production and characterization of ultrapure water for microanalysis and microchemistry. *Mikrochim. Acta* **1981**, *76*, 277–288.

(12) Seinfeld, J. H.; Pandis, S. N. *Atmospheric Chemistry and Physics: From Air Pollution to Climate Change*; John Wiley: New York, 1998.

(13) Schaber, K. Aerosol formation in absorption processes. *Chem. Eng. Sci.* **1995**, *50*, 1347–1360.

(14) Vinoj, V. *Investigation of Aerosol Characteristics over Inland, Coastal and Island Locations in India*. Ph.D. thesis, Indian Institute of Science, 2009.

(15) Weber, R.; Orsini, D.; Daun, Y.; Lee, Y.; Klotz, P.; Brechtel, F. A particle-into-liquid collector for rapid measurement of aerosol bulk chemical composition. *Aerosol Sci. Technol.* **2001**, *35*, 718–727.

(16) Vatistas, G. H.; Chen, D.; Chen, T. F.; Lin, S. Prediction of infiltration rates through an automatic door. *Appl. Therm. Eng.* **2007**, *27*, 545–550.

(17) Kumar, R.; Elizabeth, A.; Gawane, A. Air quality profile of inorganic ionic composition of fine aerosols at two sites in Mumbai City. *Aerosol Sci. Technol.* **2006**, *40*, 477–489.

(18) Wisconsin Department of Natural Resources, *Analytical Detection Limit Guidance and Laboratory Guide for Determining Method Detection Limits*; Laboratory Certification Program, PUBL-TS-056-96, 1996.

(19) Mermet, J.-M. Limit of quantitation in atomic spectrometry: An unambiguous concept? *Spectrochimica Acta Part B* **2008**, *63*, 166–182

(20) Mermet, J.-M. Calibration in atomic spectrometry: A tutorial review dealing with quality criteria, weighting procedures and possible curvatures. *Spectrochimica Acta Part B* **2010**, *65*, 509–523.

(21) Riotte, J. Private communication, 2010.